Two-phase flow and transport

C.-Y. Wang

Volume 3, Part 3, pp 337–347

in

Handbook of Fuel Cells – Fundamentals, Technology and Applications
(ISBN: 0-471-49926-9)

Edited by

Wolf Vielstich
Arnold Lamm
Hubert A. Gasteiger

Chapter 29
Two-phase flow and transport

C.-Y. Wang
The Pennsylvania State University, University Park, PA, USA

1 INTRODUCTION

Gas-liquid flow and transport is a subject of increasing importance in low-temperature proton exchange membrane (PEM) fuel cells. These fuel cells include hydrogen or reformate/air PEM fuel cells (PEMFC) and PEM-based direct methanol fuel cells (DMFC). The vast majority of currently available membranes such as Nafion require humidification in order to exhibit good proton conductivity. In addition, water is produced from the oxygen reduction reaction on the cathode. Thus, the cathode in all PEM fuel cells is susceptible to flooding, i.e., filling of pores with liquid water, especially at high current densities. Cathode flooding in DMFC is further exacerbated by the fact that a substantial amount of water can transport from the aqueous anode chamber through the membrane to the cathode side via diffusion and electro-osmotic drag. Flooding in the gas diffusion layer (GDL) and catalyst layer inhibits gaseous oxygen transport to reaction sites and blocks part of the active reaction surface, thereby representing a major obstacle to achieving high performance of PEM fuel cells. The two-phase flow and transport through the porous structure of GDL, which underlies cathode flooding, has begun to receive significant research attention.

Additionally, the two-phase flow and transport processes occur in DMFC anodes as carbon dioxide bubbles are generated from the anodic reaction of the aqueous methanol solution. The formation of CO_2 bubbles in the porous anode and their subsequent transport in, and escape from, the adjacent flow channel directly determine the activity of the anode catalyst surface and hence impact the cell performance.

Research into two-phase flow and transport in PEM fuel cells is of most recent origin. The present article is intended to summarize some initial attempts toward developing a fundamental understanding of the two-phase phenomena occurring in PEM fuel cells. Section 2 focuses on the fundamentals of two-phase flow characteristics in a fuel cell GDL. Two-phase flow occurring in flowfield channels and its interactions with the GDL are not touched here as this involves discussing a large body of relevant studies for non-fuel cell channels. A review of the existing literature in this area along with some recent visualization studies specifically on the two-phase flow patterns in fuel cell channels will be provided in a separate publication.

Section 3 discusses two-phase transport and electrochemical coupled models for PEMFC and DMFC, respectively, and illustrates their predictive capabilities and future extensions. Section 4 describes selective results using a current density distribution measurement technique to delineate the occurrence of cathode flooding. Section 5 presents a representative set of model-experiment comparisons that are illustrative of the current state of our capabilities to understand and predict two-phase phenomena in PEM fuel cells. The last section points out where challenges lie in leading to a new generation of PEM fuel cell models.

2 GDL CHARACTERIZATION AND TWO-PHASE FLOW PHYSICS

Figure 1 displays a scanning electron microscopy (SEM) image of a carbon-paper GDL made of Toray paper. It is clear that the GDL is a microscopically complex fibrous

Handbook of Fuel Cells – Fundamentals, Technology and Applications, Edited by Wolf Vielstich, Hubert A. Gasteiger, Arnold Lamm. Volume 3: *Fuel Cell Technology and Applications*. ISBN: 0-471-49926-9.

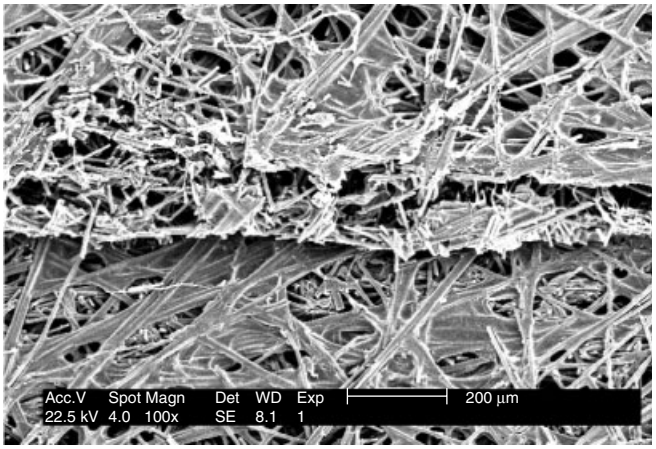

Figure 1. SEM picture of a carbon-paper gas diffusion medium.

structure with a distribution of pore sizes ranging from a few microns to tens of microns. High anisotropy is typical of the GDL. Moreover, the GDL is commonly teflonized, rendering them hydrophobic (the degree of hydrophobicity is dependent upon the amount of Teflon added to the GDL). Therefore, while the pore size, porosity, and permeability are important GDL parameters for single-phase gas flow, the surface contact angle and liquid retention are of paramount importance to two-phase flow and transport within a GDL that is governed not only by viscous forces but also by capillary forces due to the surface tension of liquid-gas interfacial meniscus present within GDL pores.

Two-phase flow and transport in a GDL is controlled largely by capillary forces as the other two forces, gravitational and viscous, are relatively small due to the small pore size and thickness of a GDL. The capillary pressure, formally defined as the difference between gas and liquid phase pressures resulting from the curved meniscus interface, thus plays a fundamental role in two-phase flow and phase distribution in a GDL. Typically the capillary pressure p_c is expressed as[1]

$$p_c = \sigma \cos\theta \left(\frac{\varepsilon}{K}\right)^{1/2} F(s) \tag{1}$$

where ε is the porosity and K the permeability of GDL, and the term $(K/\varepsilon)^{1/2}$ is characteristic of the pore length scale. The Leverett function $F(s)$ is the dimensionless capillary pressure as a function of the liquid saturation s, i.e., the volume fraction of liquid within open pores.

The contact angle θ in equation (1), defined as the angle between the liquid-gas interface and the solid surface measured at the triple point where all three phases intersect, is a quantitative measure of the wetting of GDL by a liquid. The contact angle for water on a Polytetrafluoroethylene (PTFE), or Teflon flat surface is roughly 110° (thus hydrophobic) at room temperature whereas water on the carbon surface is close to 0° (thus hydrophilic). There are two principal techniques of measuring contact angles: sessile drop method and capillary rise method (or Wihelmy gravimetric plate technique and its later version modified by Neumann).[2] Figure 2 shows an image of a water droplet on an E-Tek double-sided ELAT carbon cloth GDL at room temperature during a sessile drop experiment. The contact angle is found to be 133° from this measurement. The increased contact angle as compared to a flat surface is attributed to the surface roughness of the GDL. In general, the more appropriate method for porous GDL is the capillary rise method, especially if the contact angle becomes less than 90° at higher temperatures of actual fuel cell operation. In this method, a GDL specimen is immersed in a liquid water pool, and the capillary height h is measured as a function of time, e.g., by a traveling microscope coupled with a CCD camera. According to the wicking theory of Washburn,[3] the contact angle can be calculated from the slope of the following square-root relation between the capillary height h and elapsed time t:

$$h = \left[\frac{r_c \sigma \cos\theta}{2\tau^2 \mu}\right]^{1/2} \sqrt{t} \tag{2}$$

where r_c is the capillary radius, τ the tortuosity factor, μ the liquid viscosity, and σ the gas-liquid interfacial surface tension. The material constant $(r_c^{1/2}/\tau)$ specific to the GDL microstructure can be determined by a calibration experiment where a low surface tension liquid is used so that the contact angle may be safely assumed to be zero. Finally, the contact angle exhibits hysteresis, meaning that the advancing and receding contact angles may be very

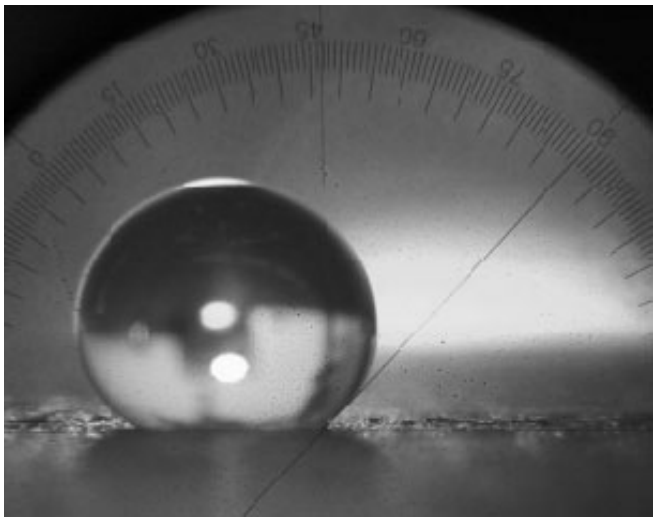

Figure 2. Drop of water on an E-Tek carbon cloth GDL at room temperature in sessile drop measurement of contact angle.

different, with the advancing contact angle being typically greater than the receding one. Such hysteresis effect is expected to play a significant role in the transient behavior of GDL flooding and therefore should be taken into account for fuel cells operating under highly dynamic conditions. Measurements of the contact angle on various common GDL and the associated hysteresis effect were presented by Lim and Wang.[4]

Another requisite two-phase parameter is the liquid retention of GDL, namely the amount of liquid "trapped" in angular corners of the pores. The liquid retention is also referred to as the irreducible liquid saturation s_{ir}, a threshold point below which the liquid becomes a discontinuous phase within the porous structure and hence remains immobile. The liquid retention can be up to 20–30% depending upon the value of $\sigma\cos\theta$.

Two-phase phenomena in a fuel cell GDL are further complicated by interactions with other interdisciplinary issues such as electrochemical reactions, electro-osmotic drag, condensation/evaporation, and multi-component diffusion. For example, exactly how liquid water blocks the "triple access" (gas reactant, electrons, protons) to each active catalyst site and hence reduces the oxygen reduction reaction rate remains largely unknown, although a directly proportional reduction of the active reaction surface with the liquid saturation is normally assumed in recent modeling efforts.[5–7] The coupling of two-phase transport in GDL and electro-osmotic drag through the membrane is also of great interest because the membrane water content increases depending on whether the membrane is in equilibrium with water vapor or liquid water. The increased water content of membrane in equilibrium with liquid water in turn results in more water molecules being dragged electro-osmotically to the cathode GDL thus leading to severe cathode flooding. Vaporization and condensation phase change takes place depending on the interplay between the local temperature and water vapor partial pressure. This phase change process impacts membrane hydration, formation of water droplets in the cathode, and/or drying of GDL by oxidant flow. Wang and Cheng presented an extensive review of these complex multiphase phenomena in general porous materials, albeit without touching upon electrochemical aspects.[1]

Liquid water forms within the cathode catalyst layer of PEM fuel cells once the local partial pressure of water vapor exceeds its saturation value. Based on this simple criterion, a threshold current density characterizing the onset of liquid water in the GDL can be estimated by:[7]

$$I_{cr} = \frac{2F}{M}\frac{\rho_{g,sat}(1 - RH_{in})}{1 + 2\alpha}\left(\frac{L}{H_{gc}}\frac{1}{u_{in}} + \frac{1}{h_m} + \frac{H_c}{D_g\varepsilon}\right)^{-1} \tag{3}$$

where F denotes Faraday constant (96 487 C mol^{-1}), M water molecular weight, $\rho_{g,sat}$ the water vapor partial density at the saturated state, RH_{in} the relative humidity at the inlet, α the net water transport coefficient through the membrane per proton, L the channel length, H_{gc} the gas channel depth, H_c the GDL thickness, u_{in} the air inlet velocity, D_g the water vapor diffusion coefficient in air, ε the GDL porosity, and h_m the mass transfer coefficient at the GDL/channel interface.

Note that the threshold current density is dependent on the water vapor diffusion resistance through the porous GDL (i.e., third term on the right-hand side of equation (3)), the mass transfer resistance at the cathode/channel interface (second term), and the ability of air in the channel to carry away water vapor by convection (first term). The threshold current density decreases with increased inlet relative humidity, channel length, and porous cathode thickness and decreased inlet velocity, operating temperature, and channel width. The net water transport coefficient is a combined result of electro-osmotic drag by electric field, fluid convection by anode/cathode pressure differential, and molecular diffusion by the concentration difference across the membrane region, thus its rigorous determination requires a full cell analysis. The GDL/channel interfacial mass transfer coefficient can be estimated approximately from the Sherwood number for laminar duct flow by:[7]

$$Sh = \frac{h_m H_{gc}}{D_g} = 2.693 \tag{4}$$

or more generally expressed as[8]

$$Sh = \frac{h_m H_{gc}}{D_g} = 1 + Pe^{\beta} \tag{5}$$

where the Peclet number, Pe, is defined as $(u_{in}H_{gc}/D_g)$, and β is an exponent that depends on the channel geometry. Equation (5) introduces a quasi-empirical macroscopic diffusion enhancement to account for gas convection at the boundary between GDL and open channel.

3 TWO-PHASE TRANSPORT AND ELECTROCHEMICAL COUPLED MODELING

Quantitative understanding and modeling of two-phase flow phenomena coupled with the electrochemical processes in PEM fuel cells will facilitate innovative design and performance improvement. There are two distinct approaches to the modeling of two-phase flow and transport in porous materials: continuum vs. pore-scale methods. Discussions

in this section are restricted to continuum modeling as the pore-scale method has not yet been applied to fuel cells.

Wang and Cheng provided a review of various continuum models for multiphase transport of mass, momentum, species and heat in porous media with and without phase change.[1] When applied specifically to PEM fuel cells, such a model treats the liquid and gas as separate phases while incorporating appropriate interfacial conditions between them (e.g., for evaporation/condensation and capillarity). The two-phase model thus consists of macroscopic conservation equations of overall mass, momentum, species, charge and energy for each individual phase, with the electrochemical reactions represented by various source terms. A generalized Darcy law is used to represent momentum conservation in each phase, with the relative permeabilities of each phase introduced to account for a decrease in the effective flow cross-section due to the presence of the other phase. Due to a large number of the field variables arising from such a mathematical description, solutions of two-phase flow problems are typically difficult, particularly under situations involving multi-dimensional effects, capillarity, and phase change. Another central difficulty lies in the presence of moving and irregular phase interface separating a single-phase (e.g., all gas region) from two-phase sub-regions that co-exist in a physical system. The location of this interface is not known a priori but must be determined by the coupled flows in the two adjacent regions. Fortunately, these numerical challenges can be circumvented by the use of a so-called multiphase mixture (M^2) formalism which was developed in the past decade and has been successfully demonstrated in solving a wide variety of multiphase flow and transport problems in porous media.[1] Based on the M^2 model, a general two-phase modeling framework for both PEMFC and DMFC was most recently created at Penn State University.[5, 7] Other research groups using the M^2 model for PEMFC included the work of You and Liu.[9] A salient feature of the M^2 model for PEM fuel cells is that the model equations are valid in all three types of regions possibly encountered in a fuel cell: all-gas, two-phase, and all-liquid. Therefore, the M^2 model provides a universal tool to simulate a reformate/air PEMFC where all gas and the gas-liquid two-phase regions are involved, as well as a DMFC in which the all-liquid state also appears within the anode chamber. The M^2 family of PEM fuel cell models predicts comprehensive information such as the phase flow fields, species concentration distributions, liquid saturation or void fraction profiles, current density distribution, and condensation/evaporation rates at the phase boundary.

Calculations have been made to simulate the two-phase distribution and transport in the air cathode based on the simplifying assumptions that the catalyst layer is an infinitely thin interface, the GDL is isotropic and homogeneous and characterized by a mean porosity and permeability, the cell temperature remains constant, and the gas phase is an ideal mixture.[7] These calculations were performed using a standard finite-volume method of Patankar, with detailed numerical procedures elaborated elsewhere.[7, 10]

A polarization curve for the air cathode portion of a hydrogen PEMFC was simulated at a cell temperature of 80 °C. The predicted curve compares well with experimental observations. At low current densities, the cathode activation overpotential is solely responsible for the potential losses of the cell. At higher current densities, more oxygen is consumed and more water is generated at the cathode-GDL/membrane interface due to both the electrochemical reaction and the water transport across the membrane from the anode. As the current density increases beyond a threshold value, i.e., $1.47\,\mathrm{A\,cm^{-2}}$ in this case, so much water is produced that its generation rate exceeds the removal rate by air from the GDL, and liquid water starts to form in the vicinity of the cathode/membrane interface. The presence of liquid water reduces the pore spaces for oxygen transport to the reaction surface as well as renders part of the surface electrochemically inactive. The cell polarization then begins to be limited by oxygen transport. An advantage of the present two-phase model is that it not only allows for two-phase analysis at higher current densities and is identically reduced to a single-phase version at low current densities where there is no liquid water, but also it predicts and ensures a smooth transition from the single- to two-phase regime of fuel cell operation. Note that this threshold current density varies with operating conditions for a given fuel cell, in particular, the cell pressure and cathode porosity as can be inferred from equation (3).

The possibility to form liquid water in the cathode of a hydrogen PEMFC is dependent on two competing rates: vapor transport rate through the GDL and the water generation rate at the catalyst layer. No liquid water will appear if water vapor can be sufficiently removed from the GDL before its partial density reaches the saturated value, e.g., $0.2907\,\mathrm{kg\,m^{-3}}$ in air at 80 °C. Figure 3(a) displays the water vapor mass fraction contours in the cathode GDL and gas channel. As air flows through the gas channel, water vapor is added from the GDL, resulting in an increased concentration downstream in the channel. This leads to a decreased concentration gradient and hence a lower water vapor diffusion rate across the GDL into the gas channel. As a result, liquid water may first appear in the vicinity of the reaction surface near the channel outlet. A two-phase zone at this location is indeed predicted in the simulation shown in Figure 3(a), where the water vapor concentration is seen to be constant at the saturated value. Figure 3(b) shows the liquid water saturation contours in the same

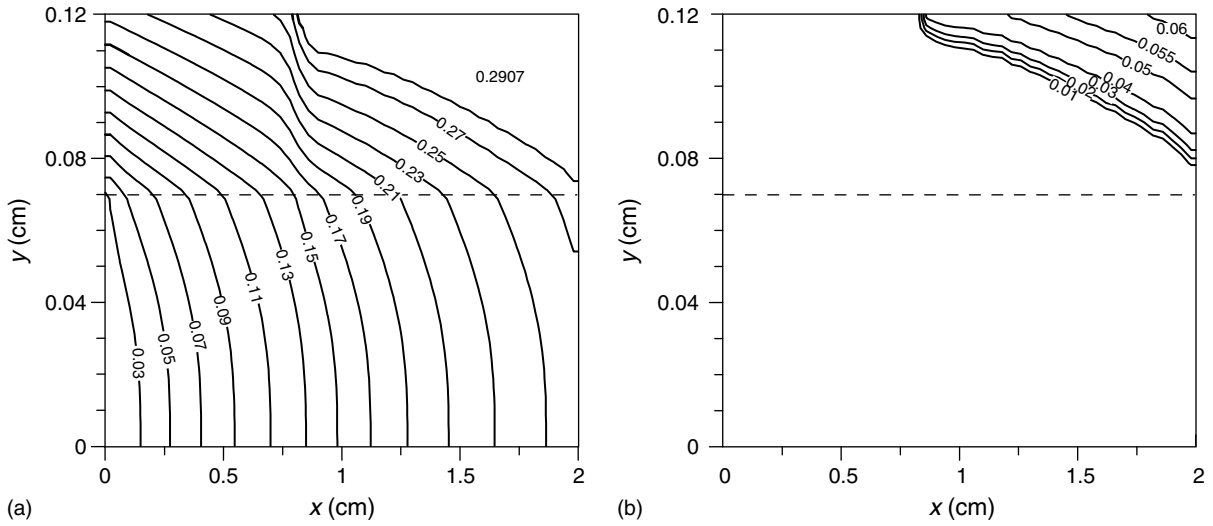

Figure 3. (a) Water vapor mass fraction, and (b) liquid water saturation distributions in the cathode GDL and channel for a dry inlet and at $1.6\,\mathrm{A\,cm^{-2}}$, $80\,^{\circ}\mathrm{C}$.[7] The x- and y-axes denote distances along and perpendicular to the flow channel, respectively, with the dashed line representing the interface between channel and GDL.

case, where liquid water is seen in the upper-right corner to coexist with the saturated water vapor. The predicted liquid amount is lower than normally observed experimentally. This is because the present simulation uses dry air at the inlet and a single channel of short length (i.e., $\sim$7 cm) as compared to typical experimental fuel cell fixtures. Also, the simulation assumed a zero contact angle which thus exaggerated the capillary-driven liquid phase transport in a real GDL. A detailed study of the contact angle effect on cathode flooding was most recently carried out by Wang and Wang.[11]

The numerical results further indicate that the gravity-induced mass flux of liquid water in the two-phase zone is less than 0.1% of that caused by capillary action. This is because the Bond number, defined as $(\rho_l - \rho_g) g H_c^2/\sigma$, is only about 0.04, implying negligible gravitational effect compared to the surface tension effect in the two-phase zone. Thus liquid water is transported mainly by capillary action to the evaporation front. The front is approximately depicted by the contour of $s = 0.01$ shown in Figure 3(b). The present simulation exemplifies the ability of M^2 model in capturing the most common scenario encountered in fuel cells, that is, a two-phase zone coexisting with a single-phase region with an irregular front in between. During transient operation, this phase front would evolve not only spatially but also temporally.

A considerable simplification to the above-described full two-phase model becomes possible if the liquid saturation within GDL is low (e.g., lower than the irreducible liquid saturation s_{ir}) or liquid droplets are too small to form a mist flow. In this situation, a single-phase approach tracking the total water amount only (i.e., make liquid water indistinguishable from water vapor) becomes valid and greatly simplifies fuel cell modeling. Based on the single-phase assumption, but otherwise carefully accounting for various water transport mechanisms within the membrane, a comprehensive three-dimensional PEMFC model has been developed and shown to be quite useful in simulating a large number of fuel cell applications.[12–14] Such a model has been used to capture three-dimensional effects resulting from complex flowfield structures, reactant bypass through the porous GDL between flow channels in a serpentine flowfield, various innovative humidification options, and CO poisoning. Figure 4 illustrates the capability of this model in the prediction of the water content distribution within the membrane for a nonhumidified case and an anode stream fully humidified case, respectively. The correlation of Springer *et al.* for the electroosmotic drag coefficient was used.[15] The first case corresponds to a portable fuel cell where the dry H_2 stream near the inlet is designed to be humidified by water transported through the membrane from the cathode exit and the humidified H_2 stream towards the exit returns water back to the dry cathode inlet. Such a counter-current feed maximizes water retention within the cell. In spite of this ingenious design, it can be seen from Figure 4(a) that the two corners of the membrane near the dry inlets remain depleted of water and the anode side of the membrane in general exhibits dryness due largely to the electro-osmotic drag of water from anode to cathode. By fully humidifying the hydrogen stream while maintaining all other conditions the same (Figure 4b), there is still depletion of water on the anode side of the membrane. This implies that back diffusing sufficient water can only occur

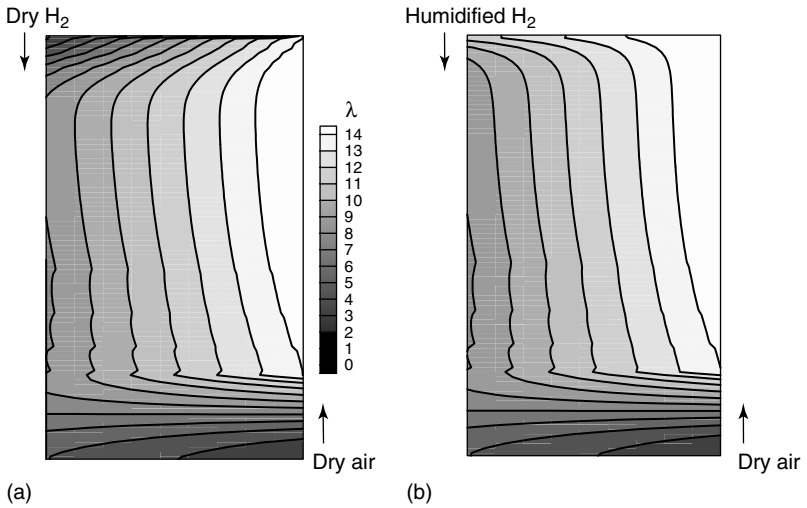

Figure 4. Water content distributions in the membrane predicted by a 3-D PEM fuel cell model: (a) in a counter-current fuel cell without external humidification, and (b) fully humidified H_2 stream but dry air.[14]

in thin membranes, i.e., thinner than Nafion 115 used in the simulations shown in Figure 4.

A 3-D simulation of flow, species, charge, and heat transport in a real-scale fuel cell using, say, a million nodes, involves the solution of roughly nine million nonlinear equations at each time step in this single-phase model. Simulations of such magnitude have been made possible with a reasonable time frame (i.e., ∼10 h of CPU on a standard PC) and thus will become routine in cell design in the near future.

For DMFC, a similar M^2 model has been formulated which considers two-phase flow and multicomponent transport in both anode and cathode. In addition, the model solves the charge transport through the membrane and fully accounts for the mixed potential effects caused by methanol oxidation at the cathode as a result of methanol crossover caused by diffusion, convection and electro-osmosis. The reader is referred to Wang and Wang for details of the DMFC two-phase model.[16] The interactions between two-phase mass transport and electrochemical kinetics in liquid-feed DMFC were explored in detail to delineate the well-known effects of methanol feed concentration and operating temperature on cell performance.[16] In particular, it was found for the first time that gas phase transport plays an important role in delivering methanol to the reaction site due to the much higher diffusion coefficient in the gas phase. This finding should have a significant implication to the design of DMFC anode GDL with suitable surface wetting characteristics.

The void fraction at the outlet of the anode flowfield can be as high as 90% and the gas and liquid phase velocities in the anode can be increased by an order of magnitude from the inlet to the outlet due to significant volume expansion. For typical DMFC (e.g., using Nafion 117), the increase in methanol feed concentration leads to a slight decrease in cell voltage but a proportional increase in the mass transport limiting current density when the methanol concentration is smaller than 1 M. At methanol concentrations greater than 2 M, the cell voltage is greatly reduced due to excessive methanol crossover and the maximum cell current density may also be limited by oxygen transport on the cathode because the parasitic reaction from methanol crossover consumes a substantial amount of oxygen as well.

Methanol crossover is found to be dominated by molecular diffusion at zero and small current densities. At high current densities, the methanol crossover flux becomes small and both the diffusion and electro-osmosis equally contribute to methanol crossover. The cell voltage can be reduced by 100 mV with methanol crossover at a small current density but the effect diminishes with increasing cell current density. The oxidation of methanol on the cathode may cause exhaustion of oxygen, thus implying that the cathode stoichiometric flow ratio cannot be at a similarly low level to the hydrogen fuel cell not only because of the need to prevent cathode flooding but also the competing consumption of oxygen between parasitic and main cathode reactions.

4 EXPERIMENTAL DIAGNOSTICS: CURRENT DISTRIBUTION MEASUREMENT

A powerful diagnostic tool to study two-phase phenomena in fuel cells and hence localized GDL flooding is the measurement of current distributions. Several groups have

attempted to create such a capability.[17, 18] These methods involve use of either a segmented MEA or a passive resistor network distributed over a full-scale cell. While these prior methods required modifications to either the MEA or the cell, this section briefly describes a nonintrusive experimental technique that was recently developed based on multi-channel potentiostat.[19] In this method, separate current collector ribs are embedded into an insulating substrate (e.g., Lexan plate) to form a segmented flowfield plate. The resulting flowfield plates for both anode and cathode are then assembled with a regular MEA to form a fuel cell with independently controllable subcells. All subcells are connected to a multi-channel potentiostat to undergo potentiostatic experiments simultaneously. The subcell currents measured thus provide information on the current density distribution for the full-scale fuel cell. The spatial and temporal resolution of this method depends on the number of channels available and capabilities of the potentiostat. Below we illustrate this technique for a DMFC, and similar results obtainable for PEMFC are not presented here for the sake of brevity.

Current density distribution measurements were made with a 50 cm^2 DMFC for a wide range of cathode flow rates in order to elucidate the nature of cathode flooding in the DMFC. Figure 5 displays the current density distributions for a high and a low cathode air flow rates, respectively. In the case of high cathode stoichiometry (Figure 5a), it can be seen that the current distributes rather uniformly for all three levels of the cell voltage. As expected, the current density increases as the cell voltage decreases. In the case of low cathode stoichiometry (but still excessive for the oxygen reduction reaction), Figure 5(b) clearly shows that a portion of the cathode towards the exit is fully flooded, leading to almost zero current. The information provided in Figure 5 can be used to identify innovative cathode flowfield designs and enables the development of MEA structures with improved water management capabilities.

5 MODEL-EXPERIMENT COMPARISONS

The current state of model-experiment comparisons can be summarized by Figure 6 for PEMFCs and by Figure 7 for DMFCs, respectively. Figure 6 display two representative cases from a large set of validation exercises that have been carried out for PEMFC in the last few years at the Penn State University Electrochemical Engine Center (ECEC) using an experimental database consisting of those published in the open literature, those experimentally measured at ECEC, and proprietary data provided by various industrial companies. Figure 6(a) demonstrates that the 3-D PEMFC model can accurately predict the current-voltage relation of a portable fuel cell without external humidification. Fuel and oxidizer are fed in countercurrent flow across the MEA in order to maintain water balance within the cell. In contrast, Figure 6(b) shows a comparison of model prediction with experiment for a fuel cell with both fuel and oxidizer streams fully humidified, a case representative of automotive fuel cells. Good agreement is achieved in both extreme cases covering a wide range of humidification conditions.

Experimental validation of a DMFC two-phase model has also been achieved for a 5 cm^2 graphite cell. A brief description of the cell geometry, MEA compositions and

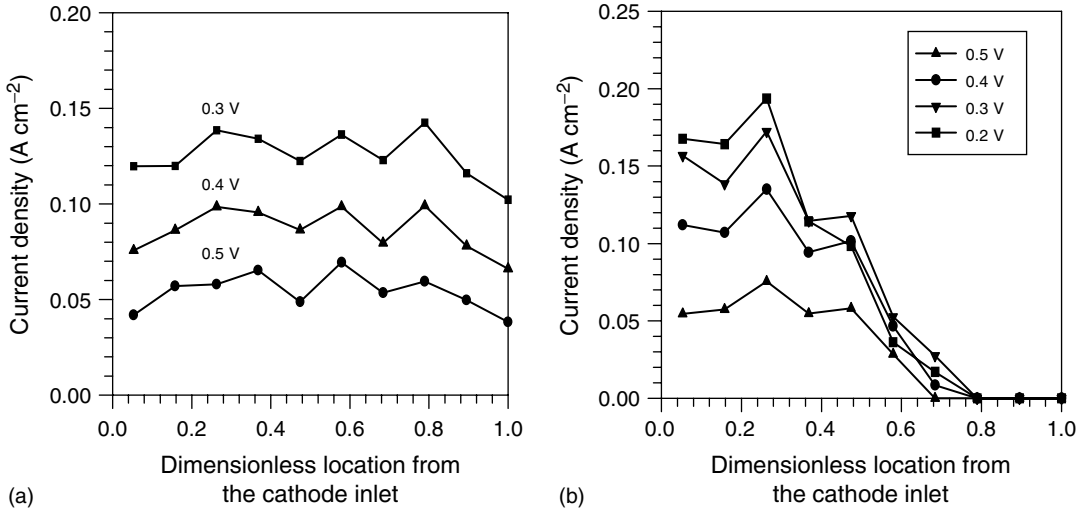

Figure 5. Current density distributions in a highly instrumented 50 cm^2 DMFC for: (a) high cathode air flowrate (stoichiometry of 85 at 0.1 A cm^{-2}), and (b) low cathode air flowrate (stoichiometry of 5 at 0.1 A cm^{-2}).[19]

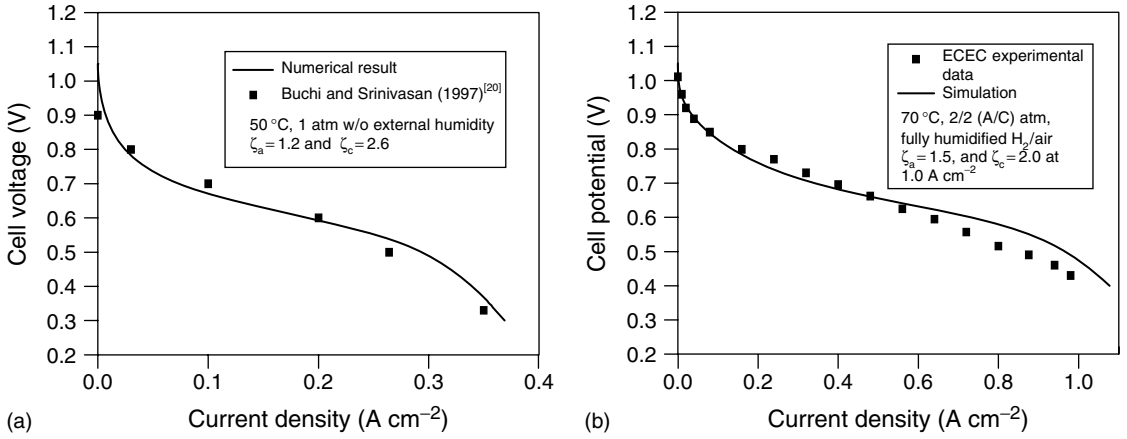

Figure 6. Comparisons of 3-D model predictions with experimental data for H_2 PEM fuel cells: (a) a portable fuel cell (50 cm^2) without external humidification of fuel and oxidizer (the experimental data were taken from[20]), and (b) an automotive fuel cell (50 cm^2) with full humidification of both fuel and oxidizer.

operating conditions is given in Figure 7(a,b). Figure 7(a) illustrates the model's capability in predicting the polarization curves at two cell temperatures. Excellent agreement is achieved not only in the kinetic- and ohmic-controlled regimes of the polarization curves but also in the mass transport controlled regime, where the methanol oxidation kinetics is modeled as a zero-order reaction for molar concentrations above 0.1 M but a first-order reaction for a molarity below 0.1 M. This shift in the reaction order and the molarity of transition are consistent with direct kinetics measurements. A lower mass transport limiting current density at 50 °C seen from Figure 7(a) is caused by the lower diffusion coefficients in both liquid and gas phases and the lower saturation methanol vapor concentration in the gas phase at lower temperatures. Using the same model and corresponding property data, Figure 7(b) shows equally satisfactory agreement in the polarization curves between numerical and experimental results for different methanol feed concentrations. In accordance with the experiments, the model prediction for the 2 M case shows a slightly lower performance (due primarily to higher methanol crossover) and an extended limiting current density.

While the model validation against cell overall performance data has been satisfactory and encouraging as evident from Figures 6 and 7, the ultimate test of

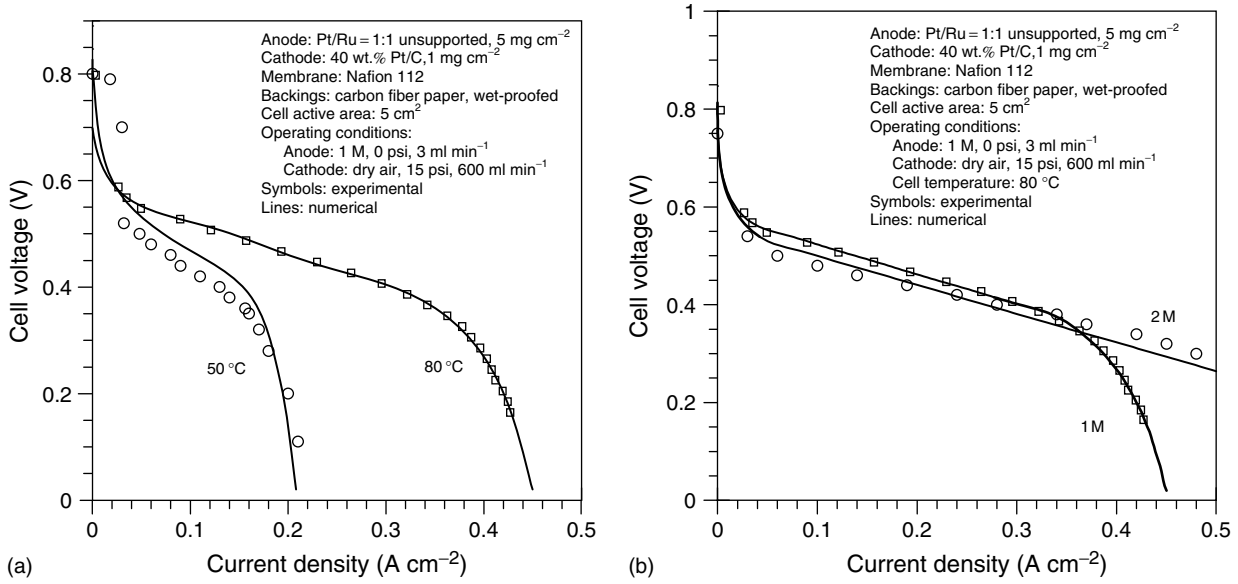

Figure 7. Comparisons of 2-D model predictions with experimental data for a DMFC with: (a) temperature effect, and (b) concentration effect.

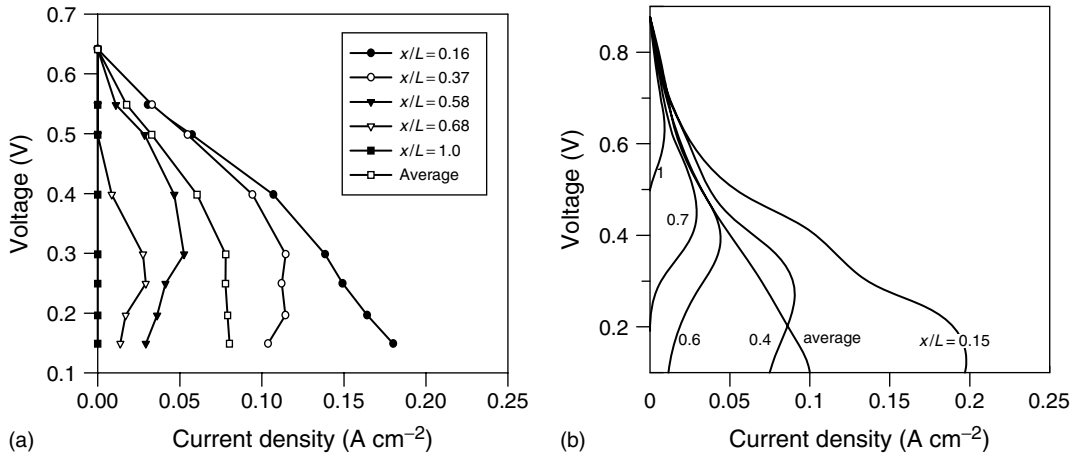

Figure 8. Comparison of localized polarization curves between experiments (a) and model predictions (b) for a 50 cm^2 DMFC with the anode flow stoichiometry of 27 and cathode air stoichiometry of 5 at 0.1 $A\,cm^{-2}$.

these highly sophisticated two-phase fuel cell models is to compare with detailed distribution measurements. Figure 8 presents such an attempt toward developing high-fidelity first-principles models for PEM fuel cells. Figure 8(a) shows a set of localized polarization curves measured via the current density distribution measurement technique described in Section 4, and Figure 8(b) displays the same set of polarization curves predicted from the DMFC two-phase model outlined in Section 3. A low air stoichiometry of 5 (but not low for the electrochemical reaction requirement) was deliberately chosen so that cathode GDL flooding may occur and a nonuniform current density distribution results.

The two graphs in Figure 8 share a striking similarity in the qualitative trend. For example, both experiment and model results indicate that the local polarization curves near the dry air inlet exhibit a monotonic function between the voltage and current. However, the shape of the polarization curves near to the exit, from both experiment and simulation, is clearly evident of flooding occurrence in the cathode GDL. Another interesting observation is that the average cell polarization curves, measured and predicted, do not exhibit any sign of cathode flooding, indicating that detailed distribution measurements are absolutely required in order to discern complex physicochemical phenomena occurring inside the cell. Finally, it can be seen from Figure 8 that a satisfactory quantitative comparison between experiment and model is still lacking on the detailed level.

Difficulties in obtaining good quantitative agreement between predicted and measured distribution results are indicative that model refinements as well as an improved property data base will be needed before accurate quantitative predictions of not only overall polarization curve but also detailed distributions within a fuel cell may be obtained. Removing uncertainties in the two-phase transport parameters that are specifically relevant to PEM fuel cells and understanding the two-phase flow phenomena in the GDL can significantly enhance the fidelity of model predictions.

6 SUMMARY AND OUTLOOK

Two-phase flow and transport in low-temperature PEM fuel cells is an important and physically rich subject. Despite that experimental and modeling capabilities are beginning to emerge, currently this is still a largely unexplored area. Much remains to be done before the knowledge of two-phase transport phenomena occurring in PEM fuel cells directly in the cell design and product development can be utilized.

Liquid phase transport in GDL by capillary action is believed to be the most important process of removing water from fuel cell cathodes. With reliable and accurate measurements of the contact angle and liquid retention within angular pores, understanding and modeling of this important process will be greatly improved.

Other two-phase flow parameters of importance include the relative permeabilities. There exist a number of empirical relations for these parameters; however, they were developed primarily by soil scientists and groundwater hydrologists, so they are most appropriate for granular materials having an aspect ratio close to unity and a relatively uniform particle size distribution. The validity of such existing relations for the relative permeabilities for fuel cell GDL therefore warrants further experimental assessment.

The complex, nonlinear mathematical system describing two-phase flow and transport problems in PEM fuel cells appears to be quite amenable numerically by the use of the

multiphase mixture (M^2) model developed a decade ago for generic multiphase transport problems in porous materials. The efficient M^2 model enables tight coupling of two-phase flow phenomena with the electrochemical processes, thus making truly three-dimensional, two-phase modeling possible for a wide range of fuel cell operating conditions. It is believed that the current modeling capabilities for two-phase flow in PEM fuel cells are more limited by the physical understanding than numerics. In addition, computational efficiency of two-phase flow codes for PEM fuel cells can further be enhanced by use of advanced numerical algorithms such as Newton-Krylov method to treat the strongly nonlinear couplings between transport and electrochemical processes as well as by the multigrid method used as an efficient linear solver. These algorithms were very successfully demonstrated for similar electrochemical systems, e.g., Li-ion cells.[21]

Finally, experimental validation is an integral part of two-phase modeling. While Section 5 clearly demonstrated that it is now possible to successfully validate these models against the cell overall performance data for both hydrogen PEMFCs and DMFCs, future focus should be placed on validation at a detailed level, e.g., comparing the current density and species concentration distributions. It is this type of detailed validation exercises that will permit an ultimate understanding of the two-phase flow phenomena in PEM fuel cells as well as development of useful tools for product design and improvement.

LIST OF SYMBOLS

D mass diffusivity
F Faraday constant
g gravitational acceleration
h height of capillary meniscus
h_m mass transfer coefficient
H geometrical dimension
I_{cr} threshold current density for the onset of liquid water in GDL
K GDL permeability
M molecular weight
p_c capillary pressure
Pe Peclet number, $u_{in}H/D_g$
r_c capillary radius
RH relative humidity
s liquid saturation, ratio of the liquid volume to the total pore volume
Sh Sherwood number, $h_m H/D_g$
t time
u velocity

Greek

α net water transport coefficient through the membrane
ε GDL porosity
μ fluid viscosity
ρ density
θ contact angle
σ interfacial surface tension
τ tortuosity factor

REFERENCES

1. C. Y. Wang and P. Cheng, 'Multiphase Flow and Heat Transfer in Porous Media' in "Advances in Heat Transfer", J. P. Hartnett Jr, T. F. Irvine, Y. I. Cho and G. A. Greene (Eds), Academic Press, New York, Vol. 30, pp. 93–196 (1997).
2. A. W. Adamson and A. P. Gast, 'Physical Chemistry of Surfaces', John Wiley & Sons, New York (1997).
3. E. W. Washburn, *Phys. Rev.*, **17**, 374 (1921).
4. C. Lim and C. Y. Wang, 'Measurement of contact angles of liquid water in PEM fuel cell gas diffusion layer (GDL) by sessile drop and capillary rise methods', Penn State University Electrochemical Engine Center (ECEC) Technical Report No. 2001–03, 2001.
5. C. Y. Wang, Z. H. Wang and Y. Pan, 'Proceedings of International Mechanical Engineering Congress & Exhibits', Nashville, TN (1999).
6. W. He, J. S. Yi and T. V. Nguyen, *AIChE J.*, **46**, 2053 (2000).
7. Z. H. Wang, C. Y. Wang and K. S. Chen, *J. Power Sources*, **94**(1), 40 (2001).
8. M. Quintard and S. Whitaker, *Adv. Water Res.*, **17**, 221 (1994).
9. L. You and H. T. Liu, in 'Proceedings of Intl. Mech. Eng. Congress and Exhibits', New York (2001).
10. S. V. Patankar, 'Numerical Heat Transfer and Fluid Flow', Hemisphere, New York (1980).
11. Z. H. Wang and C. Y. Wang, 'Cathode flooding in PEM fuel cells', *J. Power Sources*, submitted (2002).
12. S. Um, C. Y. Wang and K. S. Chen, *J Electrochem. Soc.*, **147**, 4485 (2000).
13. S. Um and C. Y. Wang, in 'Proceedings of the IMECE2000 Heat Transfer Division', ASME, Orlando, FL, Vol. 1, p. 19 (2000).
14. S. Um, 'Numerical Simulation of Water Transport and Distribution in PEM Fuel Cells', Unpublished Ph.D. Dissertation Work, Pennsylvania State University, University Park, PA (2001).
15. T. E. Springer, T. A. Zawodinski and S. Gottesfeld, *J Electrochem Soc*, **136**, 2334 (1991).
16. Z. H. Wang and C. Y. Wang, in 'Direct Methanol Fuel Cells', S. R. Narayanan, S. Gottesfeld and T. Zawodzinski (Eds),

The Electrochemical Society, Pennington, NJ, 2001–4, p. 286 (2001).

17. J. Stumper, S. A. Campbell, D. P. Wilkinson, M. C. Johnson and M. Davis, *Electrochim. Acta*, **43**, 3773 (1998).
18. S. J. C. Cleghorn, C. R. Derouin, M. S. Wilson and S. Gottesfeld, *J. Appl. Chem.*, **28**, 663 (1998).
19. M. Mench, J. Scott, S. Thynell and C. Y. Wang, 'Direct Methanol Fuel Cell Experimental and Model Validation Study', Presented at 200th Electrochemical Society Meeting, San Francisco, CA, Sep. 2–7 (2001).
20. F. N. Buchi and S. Srinivasan, *J. Electrochem. Soc.*, **144**, 2767 (1997).
21. J. Wu, V. Srivinasan, J. Xu and C. Y. Wang, *J. Electrochem. Soc.*, in press (2001).